Fault Geometry and Stress Distribution of the 2018 Mw 6.4 Hualien Earthquake in Taiwan

James Chen, Mong-Han Huang

Email: jchen24@terpmail.umd.edu
University of Maryland College Park

INTRODUCTION

Taiwan is a tectonically active region and earthquakes are not scarce, which makes it a useful location to study the interior of the earth's crust. On February 6, 2018, a Mw 6.4 earthquake occured in the city of Hualien. Hualien is located above the Milun fault, lying NE of the Longitudinal Valley Fault (LVF). Along the eastern coast of Taiwan, the Luzon Arc in the Philippine Sea Plate is obliquely colliding into the Eurasian continental boundary. The surface motion velocity vectors largely indicate a westward trend in motion due to the collision of the Philippine Sea plate into the Eurasian plate [Ching et al. 2011]. At the northern tip of the LVF, the surface velocity vectors flip from sinistral block rotation in the southern half of Taiwan to dextral rotation in the northeastern region of Taiwan.

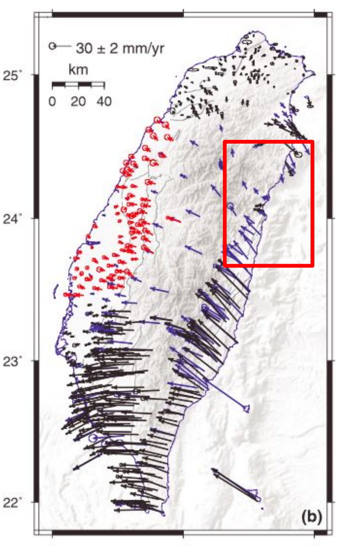

Ching et al. '11

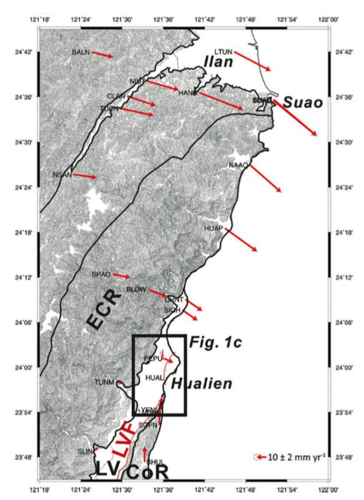

Chen et al. '08

TEC Report 2018

Geographic cross section

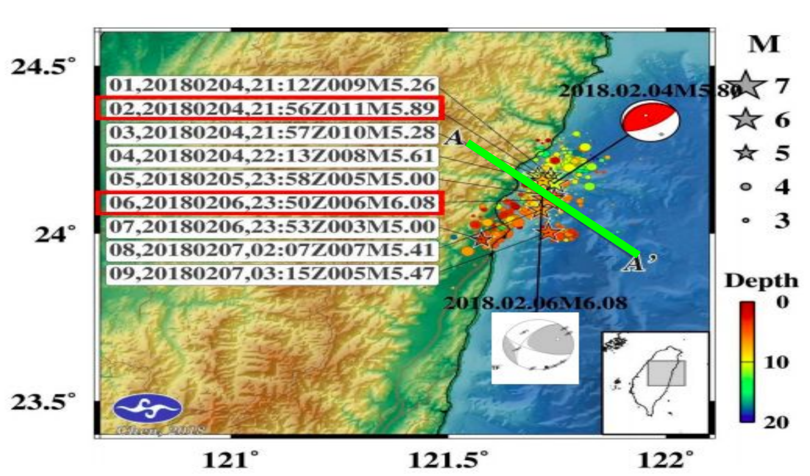

Seismicity depth profile

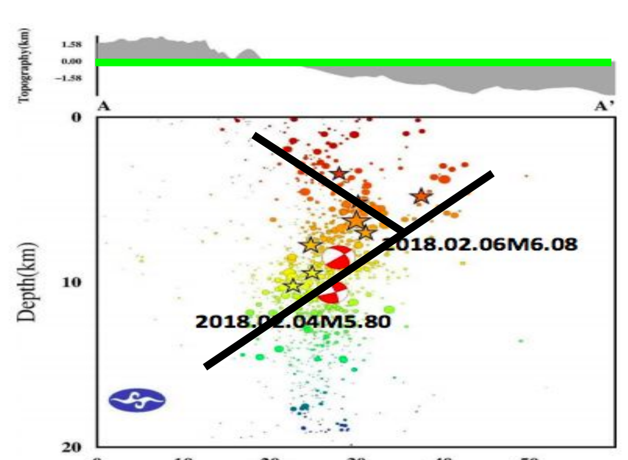

HYPOTHESIS

We propose that there is a shallower unidentified backthrust fault above the primary west dipping fault. We will be using InSAR to constrain the fault geometry in the Hualien district and a postseismic slip analysis to characterize the rheology in the northern tip of the LVF following the 2018 M_w 6.4 Hualien earthquake. We expect shallow afterslip occurring north and south of the coseismic rupture in the first month of the postseismic phase.

METHODS

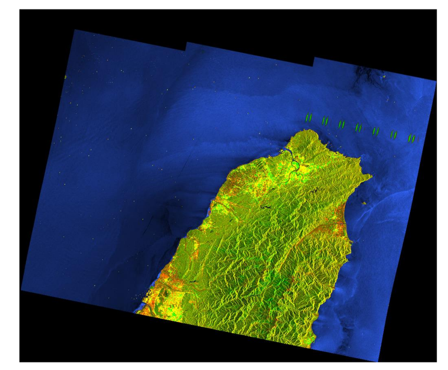

Image acquired on 2018-03-31 from Sentinel-1B. Data courtesy of ESA

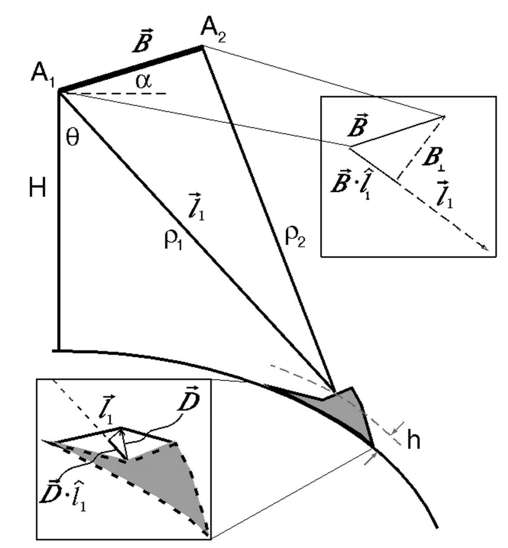

Burgmann et al. 2000

Synthetic Aperture Radar Interferometry (InSAR)

- Provides temporal evolution of 3D displacement
- Calculates relative phase difference in reference and target images

Combined coseismic and afterslip modeling

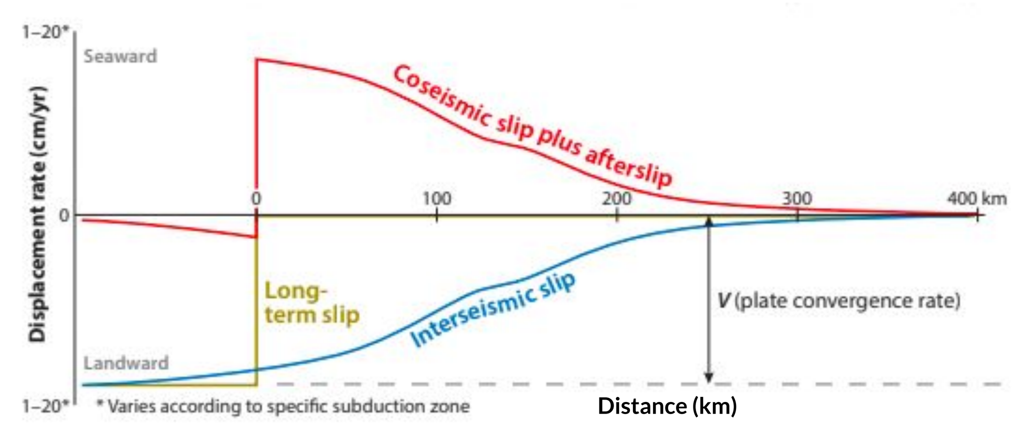

Avouac 2015

Comparing analytic solution with observed

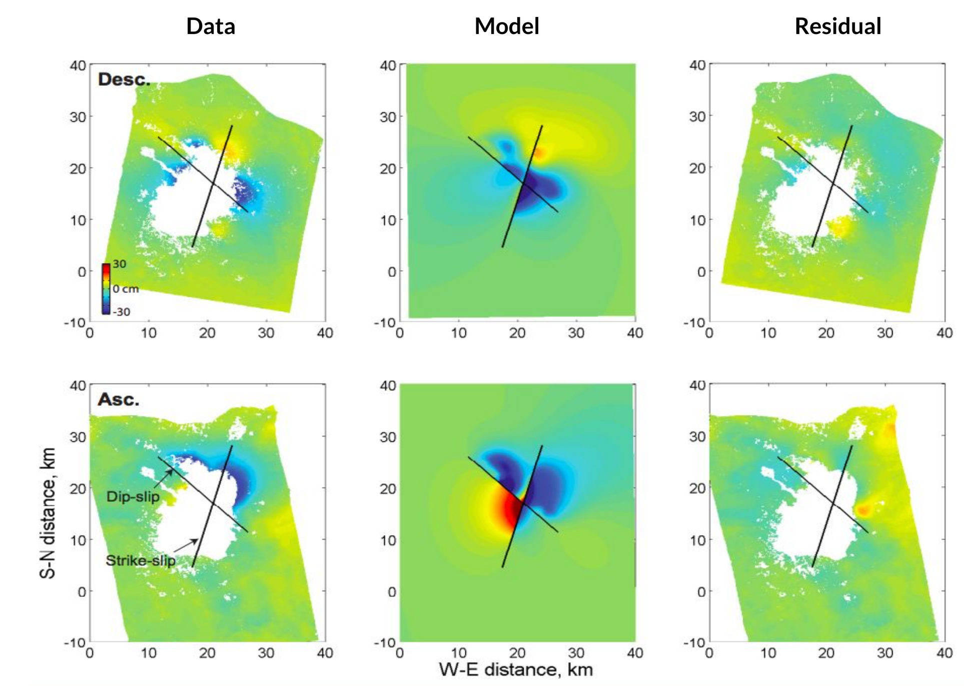

2011 Eritrea EQ, Hamiel et al. 2016

DATA

Cumulative LOS displacement

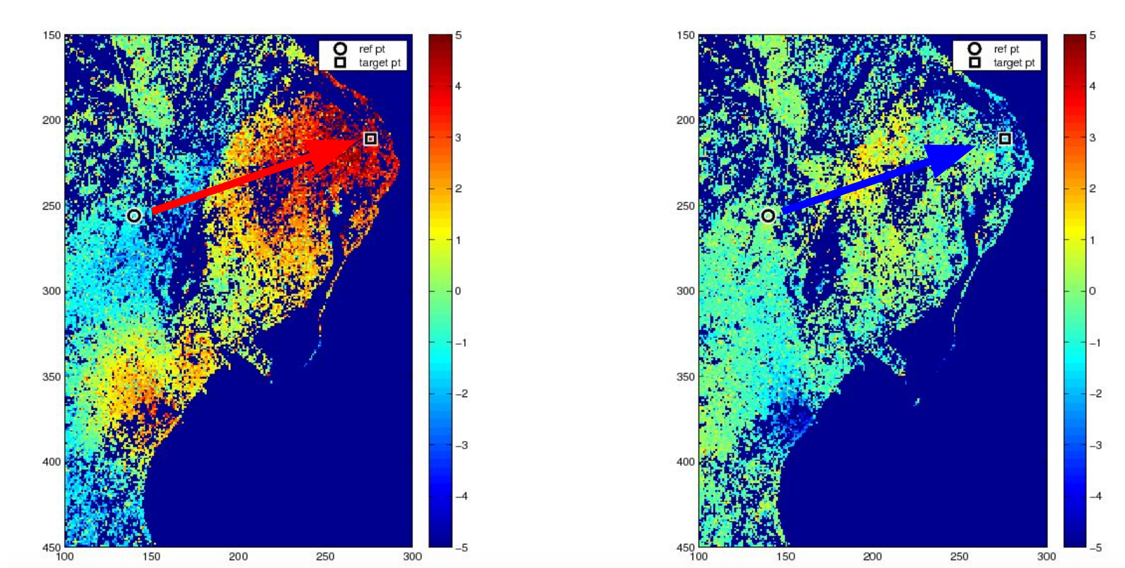

East West

Up Down

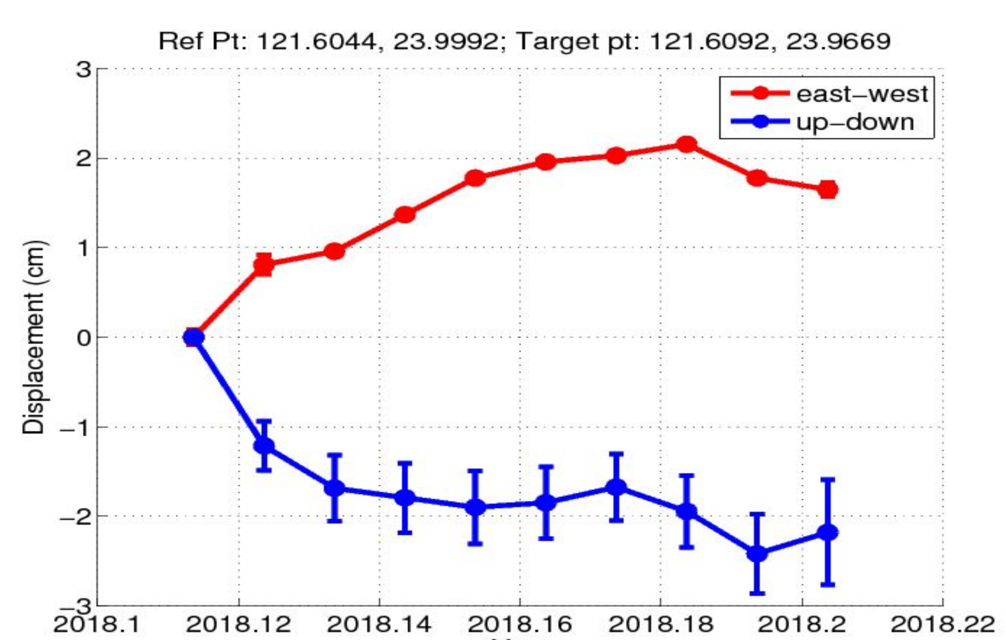

Coseismic interferogram - single pair

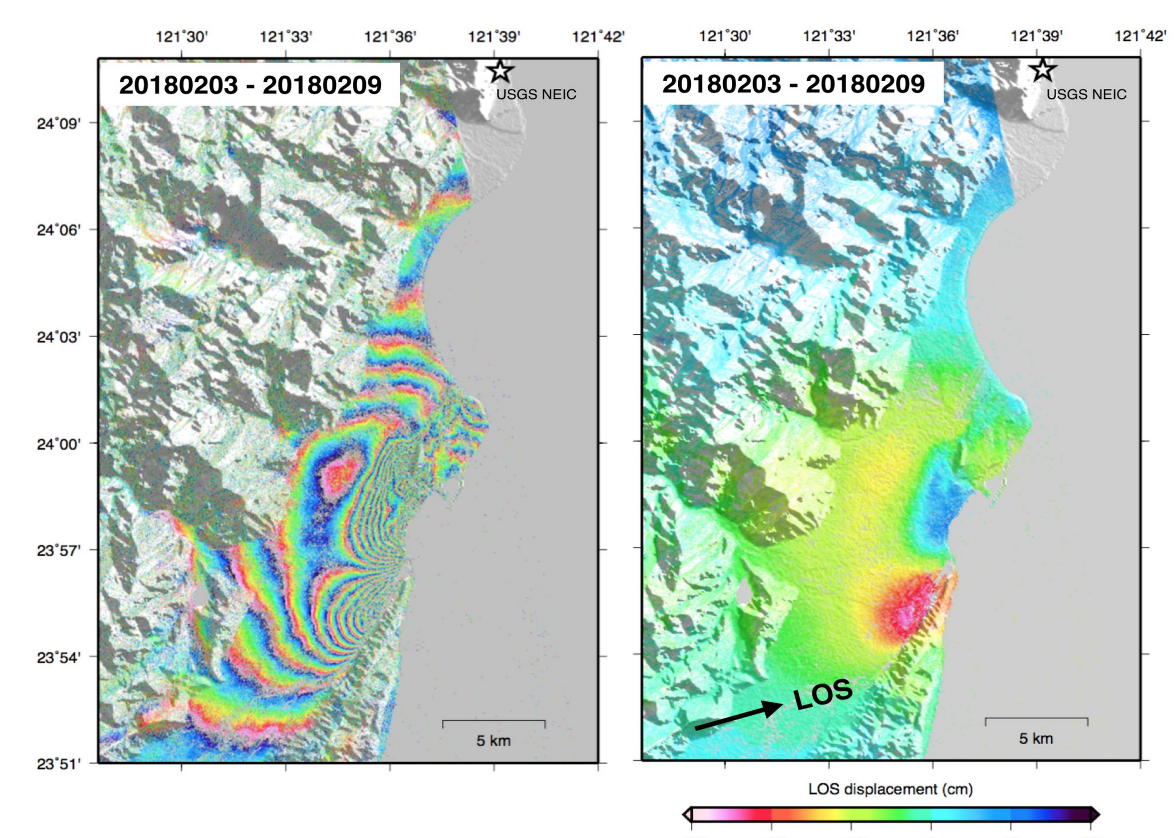

- Postseismic interferogram pairs spanning February to April 2018

FUTURE WORK

Coseismic displacement vectors

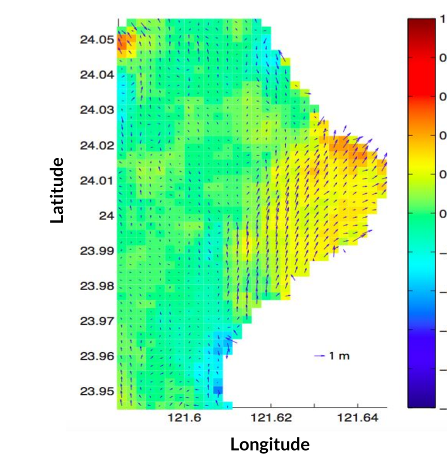

Slip inversion

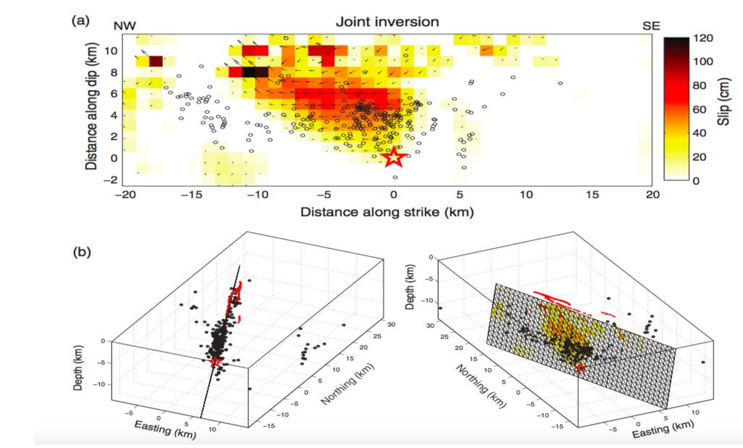

Dreger et al. 2015

- Coulomb stress changes can be analyzed following slip inversion of coseismic rupture

SUMMARY

Initial observations from the cumulative LOS displacement demonstrate a decay of displacement rate in and east/downward motion during the first two months following the 2018 Hualien earthquake. This is characteristic of oblique fault thrusting and confirms that the fault slip occurs beneath the selected cross section (blue and red arrow in afterslip observation).

However in March, a kink appears in the middle of the blue UD (Up - Down) trendline. We believe this is a result of an anomalous interferogram product from the data point corresponding to ~2018.17 years.

In the future, ascending and descending and paths will be combined to produce unwrapped interferogram. We use path 69 for ascending and path 105 for descending looks from satellites Sentinel-1A and Sentinel-1B. Currently the ascending pairs have been processed but not the descending path.

When a slip inversion is created from the seismic signal of the Hualien EQ, the Coulomb stress changes in the fault system beneath Hualien may be studied.

References

Avouac, J.-P. (2015), From Geodetic Imaging of Seismic and Aseismic Fault Slip to Dynamic Modeling of the Seismic Cycle, *Annual Review of Earth and Planetary Sciences*, 43(1), 233-271, doi:10.1146/annurev-earth-060614-105302.

Bürgmann, R., P.-A. Rosen, E.-J. Fielding (2000), Synthetic Aperture Radar Interferometry to Measure Earth's Surface Topography and Its Deformation, *Annual Review of Earth and Planetary Sciences*, 28. 169-209. 10.1146/annurev.earth.28.1.169.

Chen, C.-Y., J.-C. Lee, Y.-G. Chen, and R.-F. Chen (2014), Campaigned GPS on Present-Day Crustal Deformation in Northernmost Longitudinal Valley Preliminary Results, Hualien Taiwan, *Terrestrial, Atmospheric and Oceanic Sciences*, 25(3), 337–357, doi:10.3319/tao.2013.12.25.01(TT).

Ching, K.-E., R.-J. Rau, K. M. Johnson, J.-C. Lee, and J.-C. Hu (2011), Present-day kinematics of active mountain building in Taiwan from GPS observations during 1995–2005, *J. Geophys. Res.*, 116, B09405, doi:10.1029/2010JB008058.

Dreger, D.-S., M.-H. Huang, A. Rodgers, T. Taira, K. Wooddell (2015), Kinematic Finite-Source Model for the 24 August 2014 South Napa, California, Earthquake from Joint Inversion of Seismic, GPS, and InSAR Data. *Seismological Research Letters* ; 86(2A), 327–334, doi: https://doi.org/10.1785/0220140244

Hamlyn, J. E., D. Keir, T. J. Wright, J. W. Neuberg, B. Goitom, J. O. S. Hammond, C. Pagli, C. Oppenheimer, J.-M. Kendall, and R. Grandin (2014), Seismicity and subsidence following the 2011 Nabro eruption, Eritrea: Insights into the plumbing system of an off-rift volcano, *J. Geophys. Res. Solid Earth*, 119, 8267–8282, doi:10.1002/2014JB011395.

Huang, M.-H., personal communication